Shotgun Lipidomics Identifies Cardiolipin Depletion in Diabetic Myocardium Linking Altered Substrate Utilization with Mitochondrial Dysfunction†

Xianlin Han,*,‡,§ Jingyue Yang,‡ Hua Cheng,‡ Kui Yang,‡ Dana R. Abendschein,§,|| and Richard W. Gross‡,§,⊥,#

Division of Bioorganic Chemistry and Molecular Pharmacology, Division of Cardiology, and Departments of Medicine and Molecular Biology and Pharmacology, Washington University School of Medicine, St. Louis, Missouri 63110, and Department of Chemistry, Washington University, St. Louis, Missouri 63130

Received September 19, 2005; Revised Manuscript Received October 24, 2005

ABSTRACT: Diabetic cardiomyopathy is characterized by excessive utilization of fatty acid substrate, diminished glucose transport, and mitochondrial dysfunction. However, the chemical mechanisms linking altered substrate utilization to mitochondrial dysfunction are unknown. Herein, we use shotgun lipidomics and multidimensional mass spectrometry to identify dramatic decreases in the critical mitochondrial inner membrane lipid, cardiolipin, in diabetic murine myocardium (from 7.2 ± 0.3 nmol/mg of protein in control hearts to 3.1 ± 0.1 nmol/mg of protein in diabetic myocardium; $p < 0.001$, $n = 7$). Moreover, the direct metabolic precursor of cardiolipin, phosphatidylglycerol, was also substantially depleted (2.5 ± 0.2 nmol/mg of protein in control hearts vs 1.3 ± 0.1 nmol/mg of protein in diabetic myocardium; $p < 0.001$, $n = 7$). Similarly, glycerol 3-phosphate, necessary for the penultimate step in phosphatidylglycerol production, decreased by 58% in diabetic myocardium (from 4.9 ± 0.9 to 2.2 ± 0.3 nmol/mg of protein; $n = 4$). Since Barth's syndrome (a disorder of cardiolipin metabolism) induces mitochondrial dysfunction and cardiomyopathy, and since decreases in cardiolipin content precipitate mitochondrial dysfunction, these results provide a unifying hypothesis linking altered substrate utilization and metabolic flux in diabetic myocardium with altered lipid metabolism, cardiolipin depletion, mitochondrial dysfunction, and resultant hemodynamic compromise.

Diabetic cardiomyopathy is characterized chemically by the presence of marked alterations in the lipid composition of diabetic myocardium, altered substrate utilization, and mitochondrial dysfunction (*1*−*9*). It is widely believed that mitochondrial dysfunction and inefficient energy production are the underlying cause of hemodynamic alterations in diabetic myocardium. Maladaptive responses to persistent changes in substrate utilization (e.g., increased fatty acid uptake and decreased glucose transport) and metabolic flux lead to the accumulation of toxic lipids in diabetic myocardium (e.g., acylcarnitines, acyl-CoA, and triacylglycerols) which are thought to contribute to hemodynamic dysfunction (*2*, *3*, *6*, *8*, *9*). In early studies, we and others identified profound alterations in the lipid composition in obese and diabetic myocardium from rats which were accompanied by physiologic dysfunction (*1*, *2*). Further work clarified the importance of alterations in substrate utilization, in particular, in the increased reliance on fatty acid substrate, as an important contributor to the diastolic dysfunction present in diabetic myocardium (*1*, *8*). However, the molecular mechanisms through which altered myocardial fatty acid and glucose substrate utilization and mitochondrial dysfunction are chemically linked in the diabetic state are not understood.

Historically, inborn errors of metabolism have provided fundamental insights into the sequence of chemical events underlying a multitude of both physiological and pathophysiological processes. Traditionally, inherited disorders of metabolism have been identified through phenotypic alterations (signs, symptoms, pathology, and laboratory assessments), and the responsible chemical mechanisms have been deduced from biochemical, physiological, or genetic approaches. Recently, the development of lipidomics using mass spectrometry has provided a detailed metabolic fingerprint which can be utilized to compare alterations in the disease state of interest with those manifest in a growing body of known genetic diseases and nutritional disorders (*10*−*18*). Through comparisons of the similarities and differences of alterations in lipid profiles with known genetic diseases, in conjunction with the ever increasing knowledge of the roles of specific lipids in physiological and pathophysiological processes, significant insight into the chemical mechanisms underlying complex disease processes can be accrued (*9*, *19*−*23*). One such genetic abnormality, Barth's syndrome, results from mutations in the X chromosome located at Xq28 that is characterized clinically by neutropenia, skeletal myopathy, and cardiomyopathy. This disorder has been traced to alterations in cardiolipin metabolism (*24*−*28*) resulting in cardiolipin depletion, mitochondrial dysfunction, and cardiomyopathy.

† This work was supported by NIH Grant PO1HL57278.

* To whom correspondence should be addressed. Telephone: (314) 362-2690. Fax: (314) 362-1402. E-mail: xianlin@wustl.edu.

‡ Division of Bioorganic Chemistry and Molecular Pharmacology, Washington University School of Medicine.

§ Department of Medicine, Washington University School of Medicine.

|| Division of Cardiology, Washington University School of Medicine.

⊥ Department of Molecular Biology and Pharmacology, Washington University School of Medicine.

Department of Chemistry, Washington University.

10.1021/bi051908a CCC: $30.25
Published on Web 11/24/2005

Since Barth's syndrome is known to result in mitochondrial dysfunction and cardiomyopathy resulting from altered cardiolipin metabolism, we hypothesized that alterations in cardiolipin were present in diabetic myocardium leading to mitochondrial dysfunction and inefficient fatty acid utilization. We exploited the recent development of shotgun lipidomics with intrasource separation and multidimensional mass spectrometry (*10*−*12*, *29*) to gain insight into the types of lipid alterations present in diabetic myocardium. In shotgun lipidomics, multiple approaches including iterative back extractions to eliminate inorganic ion residues, utilization of very diluted lipid solutions through which lipid−lipid interactions can be minimized, selective ionization of specific lipid classes to reduce the overlap of molecular species, and multidimensional mass spectrometric array analyses have been employed (*11*, *12*). Through these measures, elimination of ionization suppression has been achieved.

Through the sensitivity and specificity intrinsically inherent in these techniques, we identified the chemical entities present in lipotoxic diabetic myocardium which likely underlie lipid-mediated dysfunction in the diabetic state. Specifically, the results were remarkable for a dramatic loss of the essential mitochondrial phospholipid, cardiolipin, and its direct metabolic precursor, phosphatidylglycerol. The depletion of phosphatidylglycerol and cardiolipin occurred in the presence of a marked decrease in glycerol 3-phosphate content likely resulting from the combined effects of the decreased glucose transport and the increased shunting of diunsaturated fatty acids (i.e., linoleic acid, the major aliphatic constituent present in cardiolipin) and other metabolic intermediates into triacylglycerols in diabetic myocardium. Since cardiolipin is known to be essential for physiological electron transport, efficient ATP synthesis, and the function of numerous mitochondrial inner membrane enzymes and since Barth's syndrome results in mitochondrial dysfunction and cardiomyopathy, these results identify a unifying hypothesis linking altered substrate utilization and lipid metabolism with mitochondrial dysfunction and cardiomyopathy in the diabetic state.

MATERIALS AND METHODS

Materials. Synthetic phospholipids including 1,1′,2,2′-tetramyristoylcardiolipin (T14:0 CL),[1] 1,2-dimyristoleoyl-*sn*-glycero-3-phosphocholine (14:1-14:1 PtdCho), 1,2-dipentadecanoyl-*sn*-glycero-3-phosphoethanolamine (15:0-15:0 PtdEtn), 1,2-dipentadecanoyl-*sn*-glycero-3-phosphoglycerol (15:0-15:0 PtdGro), 1,2-dimyristoyl-*sn*-glycero-3-phosphoserine (14:0-14:0 PtdSer), and 1-heptadecanoyl-2-hydroxy-*sn*-glycero-3-phosphocholine (17:0 lysoPtdCho) were purchased from Avanti Polar Lipids, Inc. (Alabaster, AL). Deuterated palmitic acid (d_3-16:0 FA) and triheptadecenoin (T17:1 TAG) were purchased from Cambridge Isotope Laboratories (Andover, MA) and Nu-Chek Prep, Inc. (Elysian, MN), respectively. Antibodies against cytochrome *c* and ATP synthase β were purchased from BD Biosciences Pharmingen (San Diego, CA). Horseradish peroxidase linked secondary antibody and ECL Western blotting detection reagent were from Amersham Bioscience (Piscataway, NJ). Glycerol-3-phosphate oxidase, glycerol-3-phosphate dehydrogenase, catalase, and NADH were obtained from Roche Applied Sciences (Indianapolis, IN). All the solvents used for sample preparation and for mass spectrometric analysis were obtained from Burdick and Jackson (Honeywell International Inc., Burdick and Jackson, Muskegon, MI). Glycerol 3-phosphate and other chemicals were purchased from Sigma-Aldrich (St. Louis, MO).

Induction of Diabetes and Sample Preparation. Male mice (C57BL/6, 4 months of age) were purchased from The Jackson Laboratory (Bar Harbor, ME). Diabetes in 15 mice was induced by a single intravenous injection (in the tail vein) of streptozotocin at 4 months of age (165 mg/kg body weight in 0.1 mL of 0.1 M citrate buffer, pH 4.5) as described previously (*2*). Control mice received citrate buffer (0.1 mL) alone. Diabetes was confirmed within 48 h by blood glucose levels >3 mg/mL as measured by chemstrips (bG; Boehringer-Mannheim). All animal procedures were performed in accordance with the Guide for the Care and Use of Laboratory Animals (National Academy of Science, 1996) and were approved by the Animals Studies Committee at Washington University. Mice were killed by asphyxiation with carbon dioxide after diabetes was induced for 4 weeks. The hearts were excised quickly and immersed in ice-cold buffer (250 mM sucrose/25 mM imidazole, pH 8.0, at 4 °C). After extraneous tissue and epicardial fat were removed, each heart was quickly dried and immediately freeze-clamped at the temperature of liquid nitrogen. Myocardial wafers were pulverized into a fine powder with a stainless steel mortar and pestle. Protein assays on the wafers were performed using a bicinchoninic acid protein assay kit (Pierce, Rockford, IL) with bovine serum albumin as a standard. A myocardial sample (approximately 10 mg) was weighed from each mouse heart, and lipids were extracted by the modified method of Bligh and Dyer (*30*) as described previously.

Internal standards including 14:0-14:0 PtdSer (1.0 nmol/mg of protein), T14:0 CL (5.0 nmol/mg of protein), 15:0-15:0 PtdGro (4.2 nmol/mg of protein), 15:0-15:0 PtdEtn (18.75 nmol/mg of protein), 14:1-14:1 PtdCho (15 nmol/mg of protein), 17:0 lysoPtdCho (1 nmol/mg of protein), T17:1 TAG (10 nmol/mg of protein), and d_3-16:0 FA (2 nmol/mg of protein) were added to each myocardial sample on the basis of protein concentration prior to extraction of lipids. Thus, the lipid content can be normalized to the protein content and quantified directly. These internal standards were selected because they represent ≪1% of endogenous cellular lipid molecular species present as demonstrated by ESI/MS lipid analysis without addition of these internal standards.

Next, the extraction mixture was centrifuged at 2500 rpm for 10 min. The chloroform layer was carefully removed and saved. To the MeOH/H_2O layer of each test tube was added an additional 2 mL of chloroform, and chloroform layer was separated as above. The chloroform extracts from each identical sample were combined and dried under a nitrogen stream. Each individual residue was then resuspended in 4 mL of chloroform/methanol (1:1) and reextracted against 1.8 mL of 20 mM LiCl aqueous solution, and the extract was

[1] Abbreviations: CL, cardiolipin; ESI, electrospray ionization; *m*:*n*, acyl chain containing *m* carbons and *n* double bonds; MS, mass spectrometry; NL, neutral loss; PC, choline glycerophospholipids; PE, ethanolamine glycerophospholipids; PI, precursor ion; PlsEtn, plasmenylethanolamine(s); PtdCho, phosphatidylcholine(s); PtdEtn, phosphatidylethanolamine(s); PtdGro, phosphatidylglycerol(s); PtdIns, phosphatidylinositol(s); PtdSer, phosphatidylserine(s); SM, sphingomyelin(s); TAG, triacylglycerol; T*m*:*n* TAG, tri *m*:*n* glycerol.

dried as described above. Individual residues were resuspended in ~1 mL of chloroform and filtered with a 0.2 μm PFTE syringe filter into a 5 mL glass centrifuge tube (this step was repeated twice). The chloroform solution was subsequently dried under a nitrogen stream, and each individual residue was reconstituted with a volume of 500 μL/mg protein (which was based on the original protein content of the samples as determined from protein assays) in 1:1 chloroform/methanol. The lipid extracts were finally flushed with nitrogen, capped, and stored at −20 °C for ESI/MS (typically analyzed within 1 week). Each lipid solution was further diluted approximately 50-fold just prior to infusion and lipid analysis. To the diluted lipid solutions was added LiOH (50 nmol/mg of protein) immediately prior to performing further lipid analyses in both negative- and positive-ion modes.

Instrumentation and Mass Spectrometry. A triple-quadrupole mass spectrometer (ThermoElectron TSQ Quantum Ultra, San Jose, CA) operating under an Xcalibur software system was utilized in this study. The first and third quadrupoles serve as independent mass analyzers while the second quadrupole serves as a collision cell for tandem mass spectrometry. The spray voltage was maintained at −3 kV in the positive-ion mode and +3 kV in the negative-ion mode. An offset voltage on the ion transfer capillary was set to 17 V and −17 V in positive- and negative-ion modes, respectively. The heater temperature along the ion transfer capillary was maintained at 250 °C. The sheath gas (nitrogen) pressure was 2 psi. The diluted lipid extract solution was directly infused into the ESI source at a flow rate of 4 μL/min with a syringe pump. Typically, a 1 min period of signal averaging in the profile mode was employed for each MS spectrum. For tandem mass spectrometry, a collision gas pressure was set at 1.0 mTorr, but the collision energy was varied with the classes of lipids as described previously (*29*). The tandem mass spectrometry in the neutral loss (NL) mode was performed through coordinately scanning both the first and third quadrupoles with a mass difference (i.e., neutral loss) while collision activation was performed in the second quadrupole. The tandem mass spectrometry in the precursor-ion (PI) mode was performed through scanning the first quadrupole in the mass range of interest and monitoring the third quadruple for an ion of interest while collision activation was performed in the second quadrupole. Typically, a 2 min period of signal averaging in the profile mode was employed for each tandem MS spectrum. All of the MS spectra and tandem MS spectra were automatically acquired by a custom sequence subroutine operated under the Xcalibur software. Data processing of two-dimensional mass spectrometric analyses including ion peak selection, data transferring, peak intensity comparisons, and quantitation was conducted as previously described (*29*) using MicroSoft Excel Macros.

Western Blotting Analysis of Mitochondrial Proteins. The liquid nitrogen frozen mouse hearts harvested as described above were pulverized into a wafer powder. Lysate buffer (phosphate-buffered saline, pH 7.2, 1% Nonidet P-40, 0.5% sodium deoxycholate, 0.1% SDS, 30 mg/mL of aprotinin, and 0.1 mg/mL of PMSF) was added at a ratio of 5 mL/g of tissue. The tissue was disrupted and homogenized by sonication at 4 °C in a water bath sonicator for 5 min and shearing through a 22 gauge needle 10 times. The homogenized tissue was incubated at 4 °C for 30 min before being centrifuged at 10000*g* for 10 min. The supernatant was saved and used as the protein extract from the tissue.

An equal amount of proteins (based on the results of protein assays) from mouse heart homogenates of both diabetic and control mice were analyzed by SDS−PAGE. The separated protein bands were transferred to immobilon-P membranes. Nonspecific binding sites were blocked by powdered milk [5% (w/v)] prior to incubation with primary antibodies (anti-cytochrome *c* and anti-ATP synthase β). Horseradish peroxidase linked secondary antibody was used in combination with an ECL detection system to visualize immunoreactive bands.

Measurement of Glycerol 3-Phosphate Mass Content in Myocardium. Glycerol 3-phosphate was extracted from frozen mouse hearts by methanol and chloroform as previously described (*31*). Briefly, ice-cold methanol/chloroform (2:1 v/v) was added to the pulverized tissue at a ratio of 6 mL/mg of tissue. The mixture was kept on ice for 10 min to allow the tissue to thaw before addition of chloroform/water (1:2 v/v) at a ratio of 3 mL/mg of tissue. After sonication for 5 min at 4 °C and vortexing, the mixture was centrifuged at 14000*g* for 20 min at 4 °C. The upper phase was saved and dried under a stream of nitrogen. The dried residue was resuspended into 100 μL of water and used for analysis of glycerol 3-phosphate.

Glycerol 3-phosphate content was determined by an enzymatic assay system with minor modifications (*32*). Specifically, 10 μL of the diluted extract or glycerol 3-phosphate standard (0−25 μM) was mixed with 40 μL of assay buffer (200 mM tricine/KOH, pH 8, 10 mM $MgCl_2$) and incubated at 95 °C for 20 min to destroy dihydroxyacetone phosphate. The samples were cooled on ice, centrifuged, and transferred to a 96-well microplate. An additional 40 μL of assay buffer (50 mM tricine/KOH, pH 8, and 10 mM $MgCl_2$ containing 2 units of glycerol-3-phosphate oxidase, 130 units of catalase, 0.4 unit of glycerol-3-phosphate dehydrogenase, and 0.06 μmol of NADH) was added prior to incubation at 30 °C for 20 min. The absorbance at 340 nm was measured, and a standard curve of the absorbance versus the concentration of glycerol 3-phosphate was derived. The amount of glycerol 3-phosphate in the sample was determined by comparing the absorbance of the sample to the standard curve.

Miscellaneous. Protein concentration was determined with a bicinchoninic acid protein assay kit (Pierce, Rockford, IL) using bovine serum albumin as a standard. Data from biological samples were normalized to the protein content, and all data are presented as the mean ± SEM of $n = 7$ for lipid analyses and $n = 4$ for determination of glycerol 3-phosphate content. Statistical differences between mean values were determined by nested ANOVA analysis.

RESULTS

Shotgun Lipidomics Using 2D Mass Spectrometry To Identify Alterations of Cardiolipin Molecular Species in Control and Diabetic Mouse Myocardium. Recent studies have underscored the role of lipotoxicity and mitochondrial dysfunction in the pathophysiology of diabetic cardiomyopathy. However, the biochemical mechanisms underlying these alterations are incompletely understood. To determine

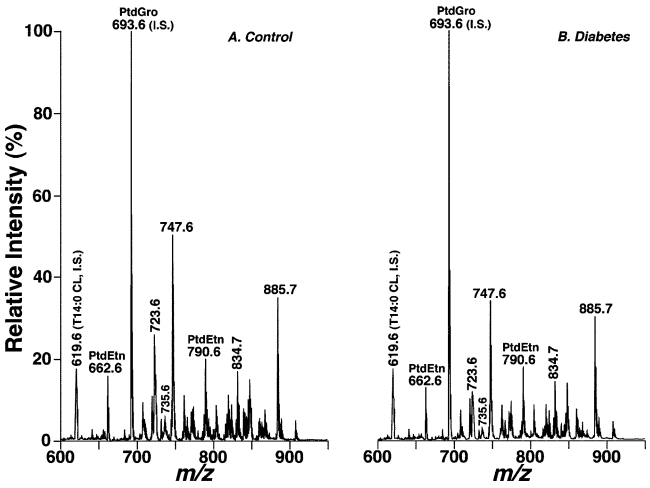

FIGURE 1: Representative negative-ion electrospray ionization mass spectra of myocardial lipid extracts from control and diabetic mice. Lipids were extracted from myocardium of a control (panel A) or diabetic (panel B) mouse by a modified Bligh and Dyer procedure. Negative-ion ESI/MS of diluted mouse myocardial lipid extracts were performed as described in Materials and Methods. The peaks of the predominant molecular species of cardiolipin (tetra 18:2, *m*/*z* 723.6) and phosphatidylglycerol (16:0-18:1, *m*/*z* 747.6) were substantially depleted in the diabetic state. Molecular species of other negatively charged phospholipids including 18:0-20:4 PtdIns (*m*/*z* 885.7) or zwitterionic phospholipids such as 18:0-22:6 PtdEtn (*m*/*z* 790.6) were not significantly depleted.

alterations in the lipidome of murine myocardium in diabetes and their potential physiological sequelae, we examined chloroform extracts of myocardium from control and diabetic mice by recently developed shotgun lipidomics and multidimensional mass spectrometry approaches. First, ESI/MS spectra acquired by direct infusion of diluted mouse myocardial lipid extracts in the negative-ion mode displayed specific differences in the lipid profiles of control and diabetic mice (compare panels A and B of Figure 1). Although similar groups of peaks were present in both the control and diabetic samples, close inspection of the first-dimensional spectra identified substantial differences in the ratios of the specific peak intensities of ions (e.g., *m*/*z* 723.6) normalized to internal standards. However, examination of the first dimension alone does not identify either the specific class or molecular species which gave rise to these ion peaks. Application of 2D mass spectrometry clearly identified the peak at *m*/*z* 723.6 crossing with a peak in the precursor-ion scanning of *m*/*z* 153 (corresponding to a phosphoglycerol derivative) and a peak in the precursor-ion scanning of *m*/*z* 279.2 (corresponding to linoleate) (Figure 2). Thus, analyses of these peaks from the molecular ion using 2D mass spectrometry unambiguously identified the peak at *m*/*z* 723.6 as doubly charged tetra 18:2 cardiolipin. In addition, several minor cardiolipin molecular species including 18:2-18:2-18:2-18:1 (peak at *m*/*z* 724.6 as its doubly charged ion, Figure 2), 18:2-18:2-18:2-20:4 (peak at *m*/*z* 735.6 as its doubly charged ion, Figure 2), and 18:0-18:2-18:2-20:4 (peak at *m*/*z* 737.6 as its doubly charged ion) were also identified. Repetitive sample analyses and comparisons of peaks with internal standards demonstrated a loss of cardiolipin mass from 7.2 $\pm$ 0.3 nmol/mg of protein in control hearts to 3.1 $\pm$ 0.1 nmol/mg of protein in diabetic hearts ($n = 7$, Figure 3A).

Mass Spectrometric Analyses of Phosphatidylglycerol, the Direct Metabolic Precursor of Cardiolipin. Furthermore, first-dimensional spectra also demonstrate a substantial decrease in peak intensity of the ion at *m*/*z* 747.6 in analysis of lipid extracts of diabetic mouse myocardium in comparison to that from controls (Figure 1). Again, application of 2D mass spectrometry demonstrated that the peak at *m*/*z* 747.6 gave rise to glycerol phosphate (precursor-ion scanning of *m*/*z* 153), palmitate (precursor-ion scanning of *m*/*z* 255.2), and oleate (precursor-ion scanning of *m*/*z* 281.2) (Figure 2). Therefore, this molecular ion was identified as deprotonated 16:0-18:1 PtdGro. Similarly, a loss of PtdGro mass from 2.5 $\pm$ 0.2 nmol/mg of protein in control hearts to 1.3 $\pm$ 0.1 nmol/mg of protein in diabetic heats was present (Figure 3B). However, only modest losses of phosphatidylinositol (from 2.4 $\pm$ 0.3 to 1.8 $\pm$ 0.5 nmol/mg of protein) and phosphatidylserine (from 5.8 $\pm$ 0.3 to 4.7 $\pm$ 0.4 nmol/mg of protein) were present without any differences in molecular species distribution. Among the PtdIns species present, the 18:0-20:4 molecular species accounts for >75% of the mass content in this class with minor amounts of 16:0-20:4, 18:1-18:1, 18:1-20:4, and 18:0-22:6 molecular species. For PtdSer molecular species, the 18:0-22:6 PtdSer accounts for ~65% of the mass content in the class with ~20% present as 18:0-20:4 PtdSer and ~15% present as 18:0-18:1 PtdSer (Figure 2).

Assessment of Mitochondrial Inner Membrane Content in Diabetic Myocardium by Marker Enzyme Analysis. Cardiolipin is well-known to be localized to the mitochondrial inner membrane. To assess if the marked decrease in cardiolipin content in diabetic mouse myocardium is due to alterations of inner membrane mitochondrial protein mass in diabetic hearts in comparison to controls, mitochondrial marker proteins were analyzed by Western blot analysis. Figure 4A shows representative examples of Western blot analyses of cytochrome *c* and ATP synthase β from myocardial homogenates of diabetic and control mice. These Western blot analyses demonstrate that both mitochondrial inner membrane marker proteins from these preparations were present in nearly equal amounts, indicating that the alterations in cardiolipin that were observed were not due to a decreased mitochondrial inner membrane content in diabetic myocardium.

Quantification of Glycerol 3-Phosphate Present in Control and Diabetic Mouse Myocardium. In mammals, cardiolipin is synthesized by a series of sequential reactions that ultimately employ CDP-diacylglycerol as the electrophile with glycerol 3-phosphate acting as the nucleophile in a reaction catalyzed by phosphatidylglycerol phosphate synthase to lead to the penultimate metabolic precursor of cardiolipin. The mass spectrometric analyses unambiguously demonstrated not only the depletion of cardiolipin but also depletion of its direct metabolic precursor phosphatidylglycerol (Figure 3). Since phosphatidylglycerol synthesis requires utilization of glycerol 3-phosphate and CDP-diacylglycerol for synthesis of its precursor phosphatidylglycerol phosphate, and since glucose transport and glycolytic flux are attenuated in diabetic myocardium, we hypothesized that diminished levels of glycerol 3-phosphate could contribute to the conjoint depletion of phosphatidylglycerol and cardiolipin. Accordingly, we measured glycerol 3-phosphate levels in control and diabetic myocardium employing a

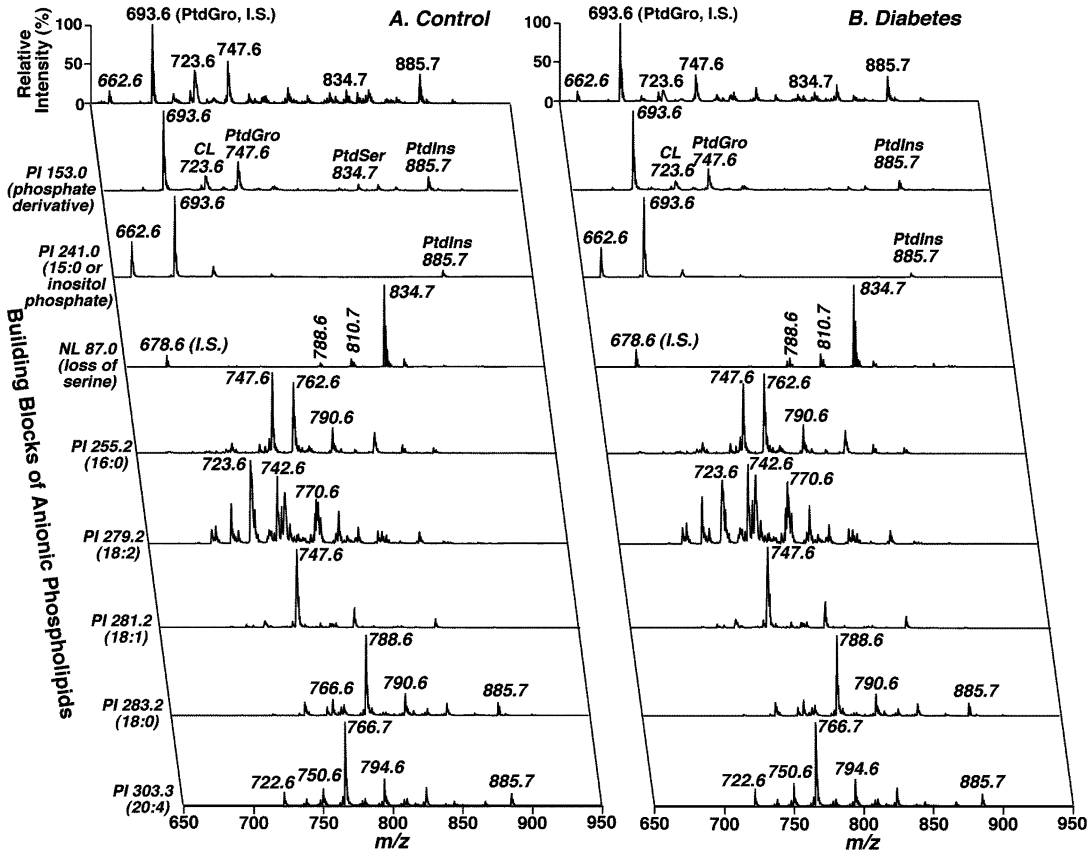

FIGURE 2: Two-dimensional electrospray ionization mass spectrometric analyses of anionic phospholipids in myocardial chloroform extracts of a control or diabetic mouse. Identical diluted lipid extracts from control (panel A) or diabetic (panel B) mice were used as described in Figure 1. Each MS or MS/MS trace of 2D ESI mass spectra was acquired by sequentially programmed custom scans operating under Xcalibur software as described in Materials and Methods. For negative-ion tandem mass spectrometry in the precursor-ion (PI) mode, the first quadrupole was scanned in the selected mass range and the second quadruple was used as a collision cell while the third quadrupole was fixed to monitor the ion of interest (i.e., either a polar headgroup of phospholipid or a fatty acyl carboxylate fragmented from anionic phospholipid molecular species). For tandem mass spectrometry in the negative-ion neutral loss (NL) mode, both the first and third quadrupoles were coordinately scanned with a mass difference (i.e., neutral loss) of 87 units, corresponding to the neutral loss of serine from phosphatidylserine molecular species, while collisional activation was performed in the second quadrupole. All mass spectral traces were displayed after normalization to the most intense peak (base peak) in each individual trace. I.S. denotes internal standard; CL represents doubly charged cardiolipin. The results demonstrate the predominance of the tetra 18:2 cardiolipin molecular species along with minor amounts of 18:2-18:2-18:2-18:1, 18:2-18:2-18:2-20:4, and 18:0-18:2-18:2-20:4 cardiolipin molecular species at *m*/*z* 724.6, 735.6, and 737.6, respectively, as their doubly charged ions.

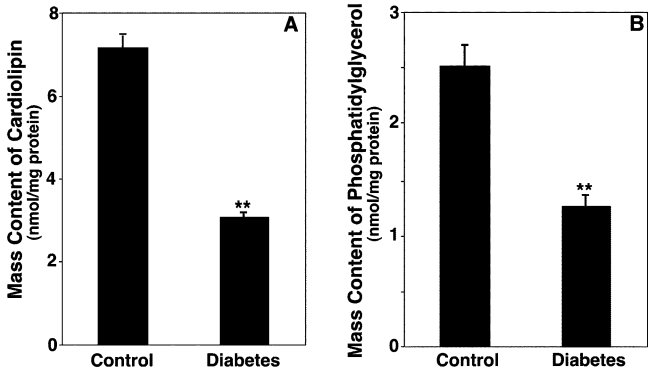

FIGURE 3: Comparison of cardiolipin and phosphatidylglycerol mass content in lipid extracts of diabetic and control mouse myocardium. Mass content of cardiolipin (panel A) and phosphatidylglycerol (panel B) was determined by multidimensional mass spectrometric array analyses by comparison of the peak intensity of each individual ion to that of the selected internal standards after corrections for ^{13}C isotopomer distribution differences as described in Materials and Methods. **, $p < 0.0001$ with $n = 7$.

spectrophotometric assay based on the conversion of NADH to NAD using an enzymatic assay system as previously described (*32*). The results demonstrated that glycerol 3-phosphate decreased from 4.9 ± 0.9 nmol/mg of protein in control myocardium to 2.2 ± 0.3 nmol/mg of protein in diabetic myocardium ($p < 0.01$, $n = 4$; Figure 4B). The data are consistent with the notion that limiting amounts of glycerol 3-phosphate contribute to the depletion of metabolites along the sequential anabolic pathway leading to cardiolipin synthesis. Collectively, these results suggest that decreased glucose transport, metabolism, or excessive removal of glycerol 3-phosphate from increased acyl-CoA levels in diabetic myocardium results in a decreased availability of glycerol 3-phosphate for use in phosphatidylglycerol and cardiolipin biosynthesis in diabetic myocardium. Thus, altered substrate supply (glucose transport), decreased metabolism (glycolytic flux), and increased metabolic shunting (removal of the residual glycerol 3-phosphate to the TAG pool) each likely play roles in the critical decrease in cardiolipin mass present in diabetic myocardium. Since cardiolipin has previously been shown to be essential for efficient mitochondrial function, these results provide an integrating hypothesis linking altered substrate utilization, lipotoxicity, and mitochondrial dysfunction in diabetic myocardium. We specifically point out that other mechanisms

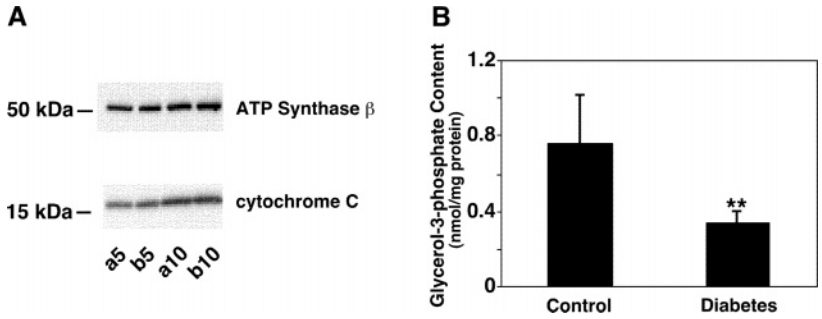

FIGURE 4: Comparison of cytochrome *c*, ATP synthase β, and glycerol 3-phosphate mass content in myocardial homogenates of diabetic and control mice. Panel A: Five (lanes a5 and b5) or 10 (lanes a10 and b10) micrograms of protein from control (lanes a5 and a10) or diabetic (lanes b5 and b10) mouse myocardium was loaded onto the gel and electrophoresed by SDS−PAGE. Proteins were transferred to PVDF membranes and subjected to Western blotting with anti-cytochrome *c* or anti-ATP synthase β antibody as described in Materials and Methods. Panel B: Glycerol 3-phosphate levels in control and diabetic myocardium were determined using a spectrophotometric assay based on the conversion of NADH to NAD in an enzymatic cycling system as described in Materials and Methods. **, $p < 0.01$, $n = 4$.

contributing to mitochondrial dysfunction are not excluded by identification of depletion of cardiolipin mass and its precursor substrates but rather that these additional mechanisms (e.g., uncoupling by fatty acids, increased free radical oxidation, etc.) could further compromise mitochondrial function in the diabetic state by additional cardiolipin depletion or through other mechanisms independent of cardiolipin depletion.

Alterations in Triacylglycerol Content and Molecular Species in Diabetic Myocardium. Traditionally, triacylglycerol accumulation in cardiac muscle has been considered a hallmark of lipotoxicity in both the obese and the diabetic states (*2*, *6*). The direct metabolic precursors of triglycerides are diglycerides which are generated from the hydrolysis of phosphatidic acid by the action of phosphatidate phosphohydrolase. It should be noted that the conversion of phosphatidic acid to diacylglycerol serves as a key branch point in lipid metabolism facilitating entry into specific types of lipid classes and molecular species. Thus, the relative kinetics of the acylation rate of diacylglycerol (resulting from phosphatidic acid) by acyl-CoA vs the condensation of phosphatidic acid with CTP to synthesize CDP-diacylglycerol leading to phosphatidylglycerol and cardiolipin (*33*) contributes to the net amount of cardiolipin synthesis in myocardium. Accordingly, alterations in the amount and the molecular species composition of TAG can provide key information on the roles of acyl-CoA and diacylglycerol acyltransferase-mediated shunting of diacylglycerol away from cardiolipin synthesis in diabetic myocardium.

To determine the types and amounts of TAG molecular species in "lipotoxic" diabetic myocardium, we exploited the 2D mass spectrometric analyses of acyl chain building blocks in TAG molecular species (Figure 5). Molecular species profiles of TAG in control and diabetic myocardial lipid extracts were substantially different (Figure 5). For example, the TAG molecular species containing arachidonate (comparison of the profiles from NL 304.3 between 2D mass spectra in Figure 5) are dramatically different. The arachidonate-containing TAG molecular species in control mice are dominated by the ion peak at *m*/*z* 885.7 while arachidonate-containing TAG molecular species in diabetic mice shifted their maximal ion peak to *m*/*z* 909.7 with other major species present at *m*/*z* 911.7 and 931.7. The total mass content of arachidonate-containing TAG molecular species increased over 4-fold from 0.24 ± 0.13 nmol/mg of protein in control mice to 1.07 ± 0.17 nmol/mg of protein. Moreover, the TAG molecular species at *m*/*z* 837.7 and 863.7 contain almost equal amounts of 16:0 acyl moieties in control myocardium whereas 16:0-containing species were predominant at *m*/*z* 863.7 and 865.7 in diabetic mice (see in the NL traces of 256.2 units in Figure 5). The results demonstrated an increase in TAG mass from 5.4 ± 0.7 nmol/mg of protein in the controls to 21.1 ± 3.5 nmol/mg of protein in diabetic mice (Table 1). This increase of 16 nmol/mg of protein of TAG was largely accounted for by 10 molecular species (16:0-18:2-18:2, 16:0-18:1-18:2, 16:1-18:1-18:1, T18:1, T18:2, 18:0-18:2-18:2, 18:1-18:2-18:2, 18:1-18:1-18:2, 16:0-18:2-22:6, and 16:0-18:1-22:6). These 10 molecular species accounted for 72 mol % of the total increase, while the 42 other measurable TAG molecular species only accounted for 28 mol % of the increased TAG mass in diabetic myocardium (Table 1).

Identification of Increased Plasmenylethanolamines in Diabetic Myocardium. Comparison of the pseudomolecular ions present in the negative-ion ESI mass spectra acquired directly from infusion of the diluted chloroform extracts of myocardium from control and diabetic mice (in the presence of LiOH) demonstrated increases in the ion peaks at *m*/*z* 746.6, 772.6, and 774.6 in diabetic myocardium which were accompanied by a concomitant decrease in the intensity of the peak at *m*/*z* 790.6 (Figure 6). Two-dimensional mass spectrometric analyses (Figure 7) identified the major peak at *m*/*z* 790.6 as 18:0-22:6 PtdEtn. In diabetic myocardium, the mass of 18:0-22:6 PtdEtn decreased from 31.1 ± 0.7 to 23.8 ± 0.3 nmol/mg of protein ($p < 0.0001$, $n = 7$). Two-dimensional mass spectrometric analyses (Figure 7) also demonstrated that ion peaks at *m*/*z* 746.6, 772.6, and 774.6 contained peaks in the precursor-ion scanning mode of *m*/*z* 327.3 (corresponding to acyl chains of 22:6). Furthermore, treatment of the lipid film with acidic vapor resulted in the disappearance of these peaks, thereby demonstrating the presence of plasmalogens and identifying these peaks as 16:0-22:6, 18:1-22:6, and 18:0-22:6 PlsEtn. Comparisons with the internal standard demonstrated that these peaks correspond to 6.9 ± 0.1, 3.5 ± 0.1, and 6.8 ± 0.1 nmol of PlsEtn/mg of protein, respectively, in control samples. Analysis of replicate samples demonstrated that this increase in plasmenylethanolamine mass was reproducible in multiple independent preparations (20.5 ± 1.4 mol % increase in diabetic myocardium; $p < 0.01$, $n = 7$).

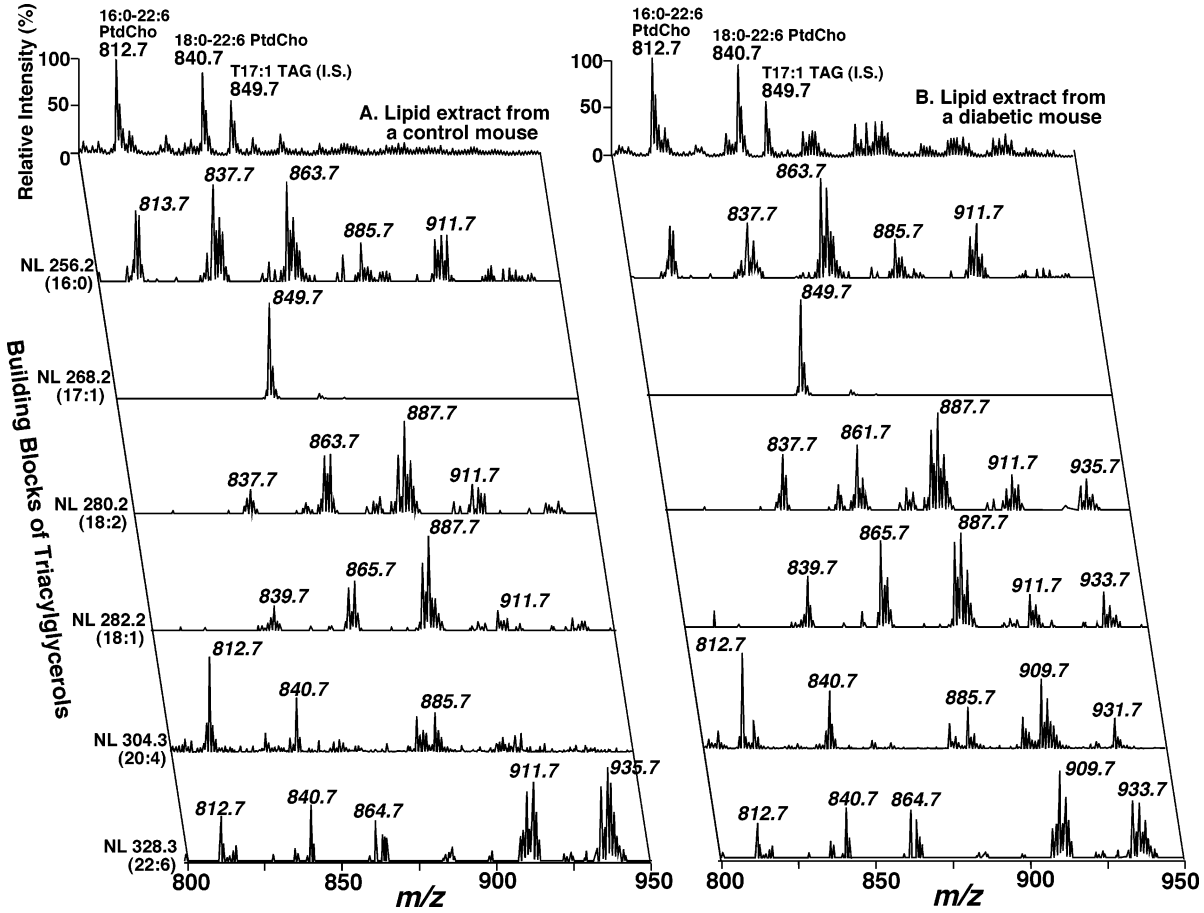

FIGURE 5: Triacylglycerol molecular species analyses by two-dimensional electrospray ionization mass spectrometry of myocardial chloroform extracts from control or diabetic mice. First-dimension spectra were obtained (top trace) in the positive-ion mode using intrasource separation. Next, neutral loss (NL) scanning of all naturally occurring aliphatic chains (i.e., the building blocks of TAG molecular species) of myocardial chloroform extracts of control (left panel) and diabetic mice (right panel) was utilized to identify the molecular species assignments, deconvolute isobaric molecular species, and quantify triacylglycerol individual molecular species by comparisons with a selected internal standard. The results were remarkable for the altered content and distribution of 20:4-containing TAG molecular species (NL scan at 304.3) in diabetic myocardium, demonstrating altered eicosanoid metabolism in the diabetic state. Each MS or MS/MS trace of 2D ESI mass spectra was acquired by sequentially programmed custom scans operating under Xcalibur software as described in Materials and Methods. For tandem mass spectrometry in the positive-ion neutral loss (NL) mode, both the first and third quadrupoles were coordinately scanned with a mass difference (i.e., neutral loss) corresponding to the neutral loss of a nonesterified fatty acid from TAG molecular species, while collisional activation was performed in the second quadrupole. All mass spectral traces were displayed after normalization to the base peak in the individual spectrum.

DISCUSSION

Recent studies have underscored the importance of alterations in lipid metabolism and resultant lipotoxicity as an underlying mechanism precipitating diastolic filling abnormalities and hemodynamic dysfunction in diabetic myocardium (*2*−*9*). In particular, the almost complete dependence on fatty acids as an energy source in diabetic myocardium is believed to contribute to mitochondrial dysfunction, although the biochemical mechanisms underlying inefficient energy production by mitochondria are not chemically defined. The 2D ESI/MS approach utilized herein led to the direct identification of a dramatic decrease in the essential mitochondrial lipid, cardiolipin, and its direct biochemical precursor, PtdGro, in diabetic myocardium. In addition, shotgun lipidomics identified 4-fold increases in the total mass of triglycerides, specific changes in triglyceride molecular species composition, and discrete alterations in the subclass and molecular species composition of ethanolamine glycerophospholipids in diabetic myocardium. Collectively, these results identify the precise chemical entities present in lipotoxic diabetic myocardium and provide insight into the biochemical mechanisms that likely contribute to mitochondrial dysfunction and cardiomyopathy in the diabetic state.

Cardiolipin is an unusual phospholipid comprised of a dimer of phosphatidate molecules linked through a glycerol backbone. Cardiolipin is localized exclusively in the mitochondrial inner membrane where it facilitates mitochondrial function through a variety of mechanisms largely related to its highly anionic character, large aliphatic chain to polar headgroup volume, and specific binding to proteins in the electron transport chain including cytochrome *c* oxidase (*34*−*37*). Depletion of cardiolipin results in release of cytochrome *c* from the mitochondrial inner membrane leading to the activation of cellular apoptosis through activation of caspase 8 (*38*, *39*). Prior work has demonstrated that palmitate overloading of cardiac myocytes induces alterations in cardiolipin content and cell death (*40*). Importantly, apoptosis has been implicated as an important mechanism of myocytic cell death in diabetic myopathy. Cardiolipin also promotes fusion of biological membranes due to its strong propensity to adapt an H_{II} hexagonal phase (*41*). In addition, the high negative charge density of the cardiolipin headgroup may

Table 1: Triacylglycerol Molecular Species and Mass Content in Lipid Extracts of Control and Diabetic Mouse Myocardium[a]

molecular species	$[M + Li]^+$	control	diabetes
16:0-16:1-18:1	837.7	0.05 ± 0.01	0.31 ± 0.06
16:0-16:0-18:2	837.7	0.07 ± 0.01	0.51 ± 0.12
16:0-16:0-18:1	839.7	0.06 ± 0.01	0.38 ± 0.02
16:0-18:2-18:2	861.7	0.45 ± 0.05	2.46 ± 0.41
16:0-18:1-18:2	863.7	0.27 ± 0.03	0.91 ± 0.16
16:1-18:1-18:1	863.7	0.37 ± 0.04	1.55 ± 0.31
16:0-18:1-18:1	865.7	0.15 ± 0.02	0.61 ± 0.11
16:1-18:0-18:1	865.7	0.04 ± 0.01	0.39 ± 0.09
T18:2	885.7	0.48 ± 0.05	2.48 ± 0.40
16:0-18:2-20:4	885.7	0.11 ± 0.01	0.20 ± 0.02
18:1-18:2-18:2	887.7	0.63 ± 0.06	3.39 ± 0.63
18:1-18:1-18:2	889.7	0.25 ± 0.03	1.42 ± 0.31
18:0-18:2-18:2	889.7	0.15 ± 0.02	1.15 ± 0.25
T18:1	891.7	0.13 ± 0.01	0.60 ± 0.06
18:0-18:1-18:2	891.7	0.03 ± 0.01	0.30 ± 0.03
16:0-18:2-22:6	909.7	0.24 ± 0.03	0.78 ± 0.13
18:2-18:2-20:4	909.7	0.03 ± 0.01	0.31 ± 0.09
16:0-18:1-22:6	911.7	0.25 ± 0.03	0.51 ± 0.06
18:1-18:2-20:4	911.7	0.07 ± 0.01	0.34 ± 0.04
18:0-18:2-20:4	913.7	0.10 ± 0.02	0.24 ± 0.06
18:2-18:2-22:6	933.7	0.21 ± 0.02	0.35 ± 0.06
18:1-18:2-22:6	935.7	0.31 ± 0.02	0.44 ± 0.04
18:1-18:1-22:6	937.7	0.19 ± 0.02	0.38 ± 0.04
total		5.38 ± 0.67	21.08 ± 3.27

[a] Mouse myocardial lipids were extracted using a modified Bligh and Dyer procedure, and the TAG molecular species in the lipid extracts were identified and quantified by using the 2D ESI mass spectrometric approach as described in Materials and Methods. The results are expressed in nmol/mg of protein and represent $X \pm$ SE of seven different animals. Only the TAG molecular species that contribute over 1% of total TAG in diabetic myocardium are listed in the table.

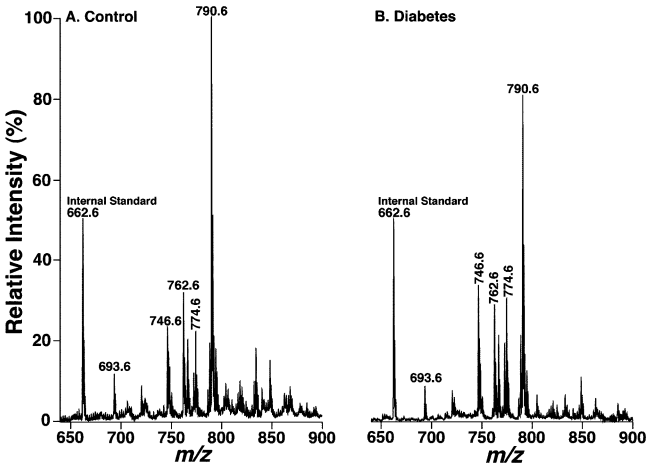

FIGURE 6: Representative negative-ion electrospray ionization mass spectra of myocardial lipid extracts from control and diabetic mice using intrasource separation. Lipid extracts from control and diabetic mice were prepared by a modified Bligh and Dyer procedure identical to those described in the legend of Figure 1. Negative-ion ESI mass spectra of diluted mouse myocardial lipid extracts in the presence of a small amount of LiOH were acquired as described in Materials and Methods. All of the abundant molecular ion peaks were identified as PE molecular species by 2D mass spectrometric analyses in Figure 7. Ion peaks at *m*/*z* 746.6, 772.6, and 774.6 are 16:0-22:6, 18:1-22:6, and 18:0-22:6 PlsEtn molecular species, respectively, whereas ion peaks at *m*/*z* 762.6 and 790.6 are 16:0-22:6 and 18:0-22:6 PtdEtn molecular species, respectively. The results demonstrate an increase in plasmenylethanolamine subclass and a decrease in phosphatidylethanolamine subclass in ethanolamine glycerophospholipids while the total mass of the ethanolamine glycerophospholipid class is essentially identical in control and diabetic myocardium.

interact with different cations and influence ion channel function. The importance of mitochondrial fusion and fission in mitochondrial function is becoming increasingly appreciated (*42*). The essential role of cardiolipin in mitochondrial function and cardiac hemodynamics has recently been underscored through identification of a genetic disorder, Barth's syndrome, in which genetic mutations in this X-linked gene (Xq28) induce altered cardiolipin metabolism, precipitate mitochondrial dysfunction, and result in a striking cardiomyopathy (*24*−*28*).

Recent studies have identified defective cardiolipin aliphatic chain remodeling in Barth's syndrome resulting in cardiolipin depletion. The causative effect of the depletion of cardiolipin content on mitochondrial and hemodynamic function is now well accepted. The pathologic decrease in cardiolipin content and altered aliphatic chain composition in Barth's syndrome has recently been shown to be initiated by the action of a mitochondrial phospholipase leading to the formation of lysocardiolipin followed by tafazzin-catalyzed transacylation to yield the predominant tetralinoleoylcardiolipin present in all known mammalian mitochondrial membranes (*43*). In Barth's syndrome, tafazzin enzymatic function is compromised, leading to cardiolipin depletion and alterations in the molecular species content of the residual cardiolipin (*44*). In the diabetic state there was dramatic cardiolipin depletion but no evidence for substantial alterations in cardiolipin molecular species content [although we cannot rule out small alterations in the relative content of the low abundance (<5%) cardiolipin molecular species]. From the dramatic effects of cardiolipin depletion on mitochondrial function documented in multiple laboratories, it seems reasonable to conclude that the dramatic loss of ~60 mol % of the cardiolipin content in the inner mitochondrial membrane demonstrated by shotgun lipidomics is responsible, at least in part, for the mitochondrial dysfunction present in diabetic myocardium.

On the basis of prior studies from multiple independent laboratories, the magnitude of cardiolipin depletion identified in this study would be predicted to result in severe defects in the kinetics and types of protein−protein interactions (e.g., complex III and complex IV supramolecular assembly) present in the mitochondrial electron transport chain. These alterations could increase uncoupling and potentially accelerate free radical generation. Moreover, the decreased efficiency of the ADP/ATP transporter (resulting in diminished chemical energy production) and decreases in the kinetics of the carnitine−acylcarnitine translocase as well as the activity of other mitochondrial inner membrane enzymes would be anticipated in the presence of this magnitude of cardiolipin depletion. It is interesting to note that impaired function of the carnitine−acylcarnitine transporter would lead to increased levels of acylcarnitine which we and others have previously observed in diabetic myocardium (*9*, *45*). Furthermore, the decrease in the inner membrane negative charge alters the surface properties of the mitochondrial inner membrane attenuating the efficiency of the transduction of transmembrane potential energy gradients into chemical energy (e.g., ATP). Accordingly, the 57% reduction in cardiolipin content observed in this study likely underlies, at least in part, the mitochondrial and hemodynamic dysfunction present in diabetic myocardium.

The loss of cardiolipin mass in diabetic myocardium is likely a multifactorial process with contributions from both

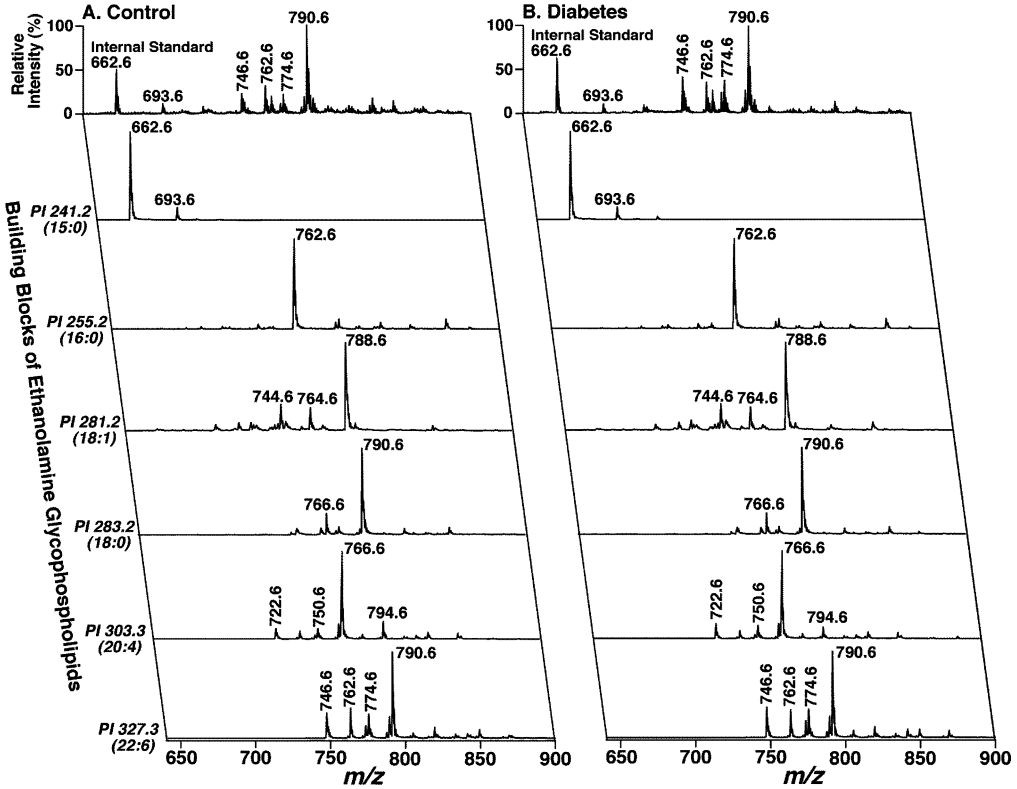

FIGURE 7: Two-dimensional electrospray ionization mass spectrometric analyses of myocardial chloroform extracts of control or diabetic mice using intrasource separation. The identical diluted lipid extracts from a control (panel A) or diabetic (panel B) mouse used for Figure 6 were employed. Each MS or MS/MS trace of 2D ESI mass spectra was acquired by sequentially programmed custom scans operating under Xcalibur software as described in Materials and Methods. For negative-ion tandem mass spectrometry in the precursor-ion (PI) mode, the first quadrupole was scanned in the selected mass range and the second quadruple was used as a collision cell while the third quadrupole was fixed to monitor the ion of interest (i.e., the fatty acyl carboxylate fragmented from PE molecular species). PE molecular species including isobaric species and regiospecificity were identified by analyses of the crossed peaks with individual building blocks of PE molecular species. All mass spectral traces were displayed after normalization to the most intense peak in each individual trace. I.S. denotes internal standard.

decreased synthesis (e.g., precursor pool depletion as demonstrated in this study) and increased cardiolipin degradation. Through multidimensional ESI/MS it is clearly demonstrated that PtdGro content is markedly decreased (Figure 1) in diabetic myocardium. Since PtdGro is the direct chemical precursor of cardiolipin, it seems likely that one, and perhaps a major, mechanism underlying cardiolipin depletion is the markedly reduced levels of phosphatidylglycerol in diabetic myocardium. Multiple independent lines of evidence demonstrate that both glucose transport and utilization are dramatically decreased in diabetic myocardium (*46*−*48*), and our results directly identify a dramatic decrease in glycerol 3-phosphate content in diabetic myocardium. Thus, the decreased levels of glycerol 3-phophate in diabetic myocardium likely contribute to PtdGro and cardiolipin depletion. One potential consequence of inappropriate reliance on fatty acid substrate at the expense of glycolysis is a decreased level of glycolytic intermediates that are necessary for providing glycerol-based metabolites for multiple different lipid synthetic pathways. Finally, lipotoxicity in diabetic myocardium results in increased levels of fatty acyl-CoA which would scavenge the available glycerol 3-phosphate, further amplifying this effect. One observation documenting alterations in the rate-limiting steps of fatty acid utilization in mitochondria is the accumulation of acylcarnitines in diabetic myocardium that we and others have previously reported (*9*, *49*).

Prior work has demonstrated the presence of increased free radical oxidation in diabetic mitochondria which can target the bisallylic hydrogen in linoleic acid, the predominant fatty acid in mammalian cardiolipin. Furthermore, intracellular linoleic acid may be sequestered during lipotoxicity by augmentation of both its absolute and relative incorporation into triglyceride molecular species as shown by 2D ESI/MS (Figure 5). Finally, supplementation with linoleic acid has salutary effects on restoring the physiologic molecular species of cardiolipin (*50*). Several types of phospholipases are located in the mitochondrial compartment, and membrane-associated phospholipases are activated in myocardium in the diabetic state (*9*). Intriguingly, the activation of one such mitochondrial calcium-independent and bromenol-sensitive phospholipase responds to alterations in the transmembrane permeability gradient which is believed to be altered in the diabetic state (*51*). Accordingly, it is likely that the combined contributions of decreased cardiolipin synthesis in conjunction with accelerated cardiolipin degradation are collectively responsible for the observed depletion of cardiolipin in diabetic myocardium and resultant mitochondrial dysfunction.

Cardiolipin depletion resulting in mitochondrial dysfunction could lead to the attenuated oxidation of fatty acids and resultant TAG accumulation found in diabetic myocardium. TAG molecular species increase dramatically in diabetic myocardium and have previously been implicated as the

etiologic agents mediating lipotoxicity (*6*). TAG could serve as a source for the generation of toxic fatty acids and fatty acyl-CoAs by hydrolysis by myocytic TAG lipases, thereby increasing the amphiphilic burden presented to diabetic myocardium. Such alterations could affect membrane dynamics and surface charge altering electromechanical coupling and the electrophysiological properties of diabetic myocardium. In addition, TAG hydrolysis would result in the production of diacylglycerol which could activate PKC-mediated signaling cascades and lead to dysfunctional metabolic or hemodynamic signaling cascades. Finally, it is also possible that the presence of TAG droplets could interfere with the flux of hydrophobic chemical constituents in myocytes or alter the mechanical properties of cardiac myocytes.

Cardiolipin depletion could also result in increased peroxisomal proliferation to accommodate the increased oxidative needs of myocardium. Concomitant with peroxisomal oxidation, the biosynthetic functions of peroxisomes such as ether lipid synthesis (a precursor of plasmalogen) could also increase. This study shows a remarkable increase in the mass content of plasmalogen molecular species. Plasmalogens alter the molecular dynamics of cell membranes and possess an increased dipole moment in comparison to their diacylphospholipid counterparts (*52*). These alterations could also influence the electrophysiological properties of myocardium and/or calcium release during contraction or reuptake during diastolic relaxation contributing to diastolic dysfunction. It is important to note that diastolic dysfunction is an important element in diabetic cardiomyopathy and that altered calcium fluxes, in part due to changes in membrane dynamics and resultant influences on transmembrane protein activities, could play an important role.

In conclusion, cardiolipin has previously been shown to be essential for physiological electron transport, inner membrane supramolecular assembly, efficient ATP synthesis, binding of cytochrome *c*, and the function of multiple other mitochondrial inner membrane enzymes. The use of shotgun lipidomics has identified cardiolipin depletion and depletion of its direct metabolic precursor, phosphatidylglycerol, thereby altering membrane charges, surface properties, and molecular dynamics. The resultant pathologic alterations in inner membrane function represent a new biochemical mechanism that integrates the altered substrate utilization present in diabetic myocardium with mitochondrial dysfunction into a unifying hypothesis. Amplification of the effects of cardiolipin depletion occurs through ineffective utilization of fatty acid substrates, resultant increases in free radical generation, and accumulation of toxic amphiphilic metabolites collectively resulting in the cardiomyopathy manifest in the diabetic state. It is our hope that these results provide a foundation for understanding the chemical mechanisms leading to diabetic cardiomyopathy.

REFERENCES

1. Lopaschuk, G. D., and Russell, J. C. (1991) Myocardial function and energy substrate metabolism in the insulin-resistant JCR:LA corpulent rat, *J. Appl. Physiol. 71*, 1302−1308.
2. Han, X., Abendschein, D. R., Kelley, J. G., and Gross, R. W. (2000) Diabetes-induced changes in specific lipid molecular species in rat myocardium, *Biochem. J. 352*, 79−89.
3. Kraegen, E. W., Cooney, G. J., Ye, J. M., Thompson, A. L., and Furler, S. M. (2001) The role of lipids in the pathogenesis of muscle insulin resistance and beta cell failure in type II diabetes and obesity, *Exp. Clin. Endocrinol. Diabetes 109* (Suppl. 2), S189−S201.
4. Finck, B. N., Lehman, J. J., Leone, T. C., Welch, M. J., Bennett, M. J., Kovacs, A., Han, X., Gross, R. W., Kozak, R., Lopaschuk, G. D., and Kelly, D. P. (2002) The cardiac phenotype induced by PPARα overexpression mimics that caused by diabetes mellitus, *J. Clin. Invest. 109*, 121−130.
5. Kelley, D. E. (2002) Skeletal muscle triglycerides: an aspect of regional adiposity and insulin resistance, *Ann. N.Y. Acad. Sci. 967*, 135−145.
6. Unger, R. H. (2002) Lipotoxic diseases, *Annu. Rev. Med. 53*, 319−336.
7. Hung, T., Sievenpiper, J. L., Marchie, A., Kendall, C. W., and Jenkins, D. J. (2003) Fat versus carbohydrate in insulin resistance, obesity, diabetes and cardiovascular disease, *Curr. Opin. Clin. Nutr. Metab. Care 6*, 165−176.
8. Finck, B. N., Han, X., Courtois, M., Aimond, F., Nerbonne, J. M., Kovacs, A., Gross, R. W., and Kelly, D. P. (2003) A critical role for PPARα-mediated lipotoxicity in the pathogenesis of diabetic cardiomyopathy: modulation by dietary fat content, *Proc. Natl. Acad. Sci. U.S.A. 100*, 1226−1231.
9. Su, X., Han, X., Mancuso, D. J., Abendschein, D. R., and Gross, R. W. (2005) Accumulation of long-chain acylcarnitine and 3-hydroxy acylcarnitine molecular species in diabetic myocardium: identification of alterations in mitochondrial fatty acid processing in diabetic myocardium by shotgun lipidomics, *Biochemistry 44*, 5234−5245.
10. Han, X., and Gross, R. W. (2003) Global analyses of cellular lipidomes directly from crude extracts of biological samples by ESI mass spectrometry: a bridge to lipidomics, *J. Lipid Res. 44*, 1071−1079.
11. Han, X., and Gross, R. W. (2005) Shotgun lipidomics: Electrospray ionization mass spectrometric analysis and quantitation of the cellular lipidomes directly from crude extracts of biological samples, *Mass Spectrom. Rev. 24*, 367−412.
12. Han, X., and Gross, R. W. (2005) Shotgun lipidomics: multidimensional mass spectrometric analysis of cellular lipidomes, *Expert Rev. Proteomics 2*, 253−264.
13. Pulfer, M., and Murphy, R. C. (2003) Electrospray mass spectrometry of phospholipids, *Mass Spectrom. Rev. 22*, 332−364.
14. Welti, R., and Wang, X. (2004) Lipid species profiling: a high-throughput approach to identify lipid compositional changes and determine the function of genes involved in lipid metabolism and signaling, *Curr. Opin. Plant Biol. 7*, 337−344.
15. Forrester, J. S., Milne, S. B., Ivanova, P. T., and Brown, H. A. (2004) Computational lipidomics: a multiplexed analysis of dynamic changes in membrane lipid composition during signal transduction, *Mol. Pharmacol. 65*, 813−821.
16. Ekroos, K., Chernushevich, I. V., Simons, K., and Shevchenko, A. (2002) Quantitative profiling of phospholipids by multiple precursor ion scanning on a hybrid quadrupole time-of-flight mass spectrometer, *Anal. Chem. 74*, 941−949.
17. Hermansson, M., Uphoff, A., Kakela, R., and Somerharju, P. (2005) Automated quantitative analysis of complex lipidomes by liquid chromatography/mass spectrometry, *Anal. Chem. 77*, 2166−2175.
18. Ishida, M., Yamazaki, T., Houjou, T., Imagawa, M., Harada, A., Inoue, K., and Taguchi, R. (2004) High-resolution analysis by nano-electrospray ionization Fourier transform ion cyclotron resonance mass spectrometry for the identification of molecular species of phospholipids and their oxidized metabolites, *Rapid Commun. Mass Spectrom. 18*, 2486-2494.
19. Han, X., Holtzman, D. M., and McKeel, D. W., Jr. (2001) Plasmalogen deficiency in early Alzheimer's disease subjects and in animal models: molecular characterization using electrospray ionization mass spectrometry, *J. Neurochem. 77*, 1168−1180.
20. Han, X., Holtzman, D. M., McKeel, D. W., Jr., Kelley, J., and Morris, J. C. (2002) Substantial sulfatide deficiency and ceramide elevation in very early Alzheimer's disease: potential role in disease pathogenesis, *J. Neurochem. 82*, 809−818.
21. Mancuso, D. J., Abendschein, D. R., Jenkins, C. M., Han, X., Saffitz, J. E., Schuessler, R. B., and Gross, R. W. (2003) Cardiac ischemia activates calcium-independent phospholipase $A_2\beta$, precipitating ventricular tachyarrhythmias in transgenic mice: rescue of the lethal electrophysiologic phenotype by mechanism-based inhibition, *J. Biol. Chem. 278*, 22231−22236.
22. Jain, S., Jayasimhulu, K., and Clark, J. F. (2004) Metabolomic analysis of molecular species of phospholipids from normotensive

and preeclamptic human placenta electrospray ionization mass spectrometry, *Front. Biosci. 9*, 3167−3175.
23. Sparagna, G. C., Johnson, C. A., McCune, S. A., Moore, R. L., and Murphy, R. C. (2005) Quantitation of cardiolipin molecular species in spontaneously hypertensive heart failure rats using electrospray ionization mass spectrometry, *J. Lipid Res. 46*, 1196−1204.
24. Vreken, P., Valianpour, F., Nijtmans, L. G., Grivell, L. A., Plecko, B., Wanders, R. J., and Barth, P. G. (2000) Defective remodeling of cardiolipin and phosphatidylglycerol in Barth syndrome, *Biochem. Biophys. Res. Commun. 279*, 378−382.
25. Schlame, M., Towbin, J. A., Heerdt, P. M., Jehle, R., DiMauro, S., and Blanck, T. J. (2002) Deficiency of tetralinoleoyl-cardiolipin in Barth syndrome, *Ann. Neurol. 51*, 634−637.
26. Valianpour, F., Wanders, R. J., Overmars, H., Vreken, P., Van Gennip, A. H., Baas, F., Plecko, B., Santer, R., Becker, K., and Barth, P. G. (2002) Cardiolipin deficiency in X-linked cardioskeletal myopathy and neutropenia (Barth syndrome, MIM 302060): a study in cultured skin fibroblasts, *J. Pediatr. 141*, 729−733.
27. Barth, P. G., Valianpour, F., Bowen, V. M., Lam, J., Duran, M., Vaz, F. M., and Wanders, R. J. (2004) X-linked cardioskeletal myopathy and neutropenia (Barth syndrome): an update, *Am. J. Med. Genet. A 126*, 349−354.
28. Gu, Z., Valianpour, F., Chen, S., Vaz, F. M., Hakkaart, G. A., Wanders, R. J., and Greenberg, M. L. (2004) Aberrant cardiolipin metabolism in the yeast taz1 mutant: a modLipidomics: a multiplexed analysis of dynamic changes in membrane lipid composition during signal tel for Barth syndrome, *Mol. Microbiol. 51*, 149−158.
29. Han, X., Yang, J., Cheng, H., Ye, H., and Gross, R. W. (2004) Towards fingerprinting cellular lipidomes directly from biological samples by two-dimensional electrospray ionization mass spectrometry, *Anal. Biochem. 330*, 317−331.
30. Bligh, E. G., and Dyer, W. J. (1959) A rapid method of total lipid extraction and purification, *Can. J. Biochem. Physiol. 37*, 911−917.
31. Le Belle, J. E., Harris, N. G., Williams, S. R., and Bhakoo, K. K. (2002) A comparison of cell and tissue extraction techniques using high-resolution ^{1}H NMR spectroscopy, *NMR Biomed. 15*, 37−44.
32. Gibon, Y., Vigeolas, H., Tiessen, A., Geigenberger, P., and Stitt, M. (2002) Sensitive and high throughput metabolite assays for inorganic pyrophosphate, ADPGlc, nucleotide phosphates, and glycolytic intermediates based on a novel enzymic cycling system, *Plant J. 30*, 221−235.
33. Bishop, W. R., and Bell, R. M. (1988) Assembly of phospholipids into cellular membranes: biosynthesis, transmembrane movement and intracellular translocation, *Annu. Rev. Cell Biol. 4*, 579−610.
34. Schlame, M., and Haldar, D. (1993) Cardiolipin is synthesized on the matrix side of the inner membrane in rat liver mitochondria, *J. Biol. Chem. 268*, 74−79.
35. Mandieau, V., Martin, I., and Ruysschaert, J. M. (1995) Interaction between cardiolipin and the mitochondrial presequence of cytochrome *c* oxidase subunit IV favours lipid mixing without destabilizing the bilayer structure, *FEBS Lett. 368*, 15−18.
36. Zhang, M., Mileykovskaya, E., and Dowhan, W. (2002) Gluing the respiratory chain together. Cardiolipin is required for supercomplex formation in the inner mitochondrial membrane, *J. Biol. Chem. 277*, 43553−43556.
37. Pfeiffer, K., Gohil, V., Stuart, R. A., Hunte, C., Brandt, U., Greenberg, M. L., and Schagger, H. (2003) Cardiolipin stabilizes respiratory chain supercomplexes, *J. Biol. Chem. 278*, 52873−52880.
38. McMillin, J. B., and Dowhan, W. (2002) Cardiolipin and apoptosis, *Biochim. Biophys. Acta 1585*, 97−107.
39. Degli Esposti, M. (2004) Mitochondria in apoptosis: past, present and future, *Biochem. Soc. Trans. 32*, 493−495.
40. Ostrander, D. B., Sparagna, G. C., Amoscato, A. A., McMillin, J. B., and Dowhan, W. (2001) Decreased cardiolipin synthesis corresponds with cytochrome *c* release in palmitate-induced cardiomyocyte apoptosis, *J. Biol. Chem. 276*, 38061−38067.
41. Ortiz, A., Killian, J. A., Verkleij, A. J., and Wilschut, J. (1999) Membrane fusion and the lamellar-to-inverted-hexagonal phase transition in cardiolipin vesicle systems induced by divalent cations, *Biophys. J. 77*, 2003−2014.
42. Bossy-Wetzel, E., Barsoum, M. J., Godzik, A., Schwarzenbacher, R., and Lipton, S. A. (2003) Mitochondrial fission in apoptosis, neurodegeneration and aging, *Curr. Opin. Cell Biol. 15*, 706−716.
43. Xu, Y., Kelley, R. I., Blanck, T. J., and Schlame, M. (2003) Remodeling of cardiolipin by phospholipid transacylation, *J. Biol. Chem. 278*, 51380−51385.
44. Vaz, F. M., Houtkooper, R. H., Valianpour, F., Barth, P. G., and Wanders, R. J. (2003) Only one splice variant of the human TAZ gene encodes a functional protein with a role in cardiolipin metabolism, *J. Biol. Chem. 278*, 43089−43094.
45. Lopaschuk, G. D., Tahiliani, A. G., Vadlamudi, R. V., Katz, S., and McNeill, J. H. (1983) Cardiac sarcoplasmic reticulum function in insulin- or carnitine-treated diabetic rats, *Am. J. Physiol. 245*, H969−H976.
46. Katz, E. B., Stenbit, A. E., Hatton, K., DePinho, R., and Charron, M. J. (1995) Cardiac and adipose tissue abnormalities but not diabetes in mice deficient in GLUT4, *Nature 377*, 151−155.
47. Stenbit, A. E., Tsao, T. S., Li, J., Burcelin, R., Geenen, D. L., Factor, S. M., Houseknecht, K., Katz, E. B., and Charron, M. J. (1997) GLUT4 heterozygous knockout mice develop muscle insulin resistance and diabetes, *Nat. Med. 3*, 1096−1101.
48. Dhalla, N. S., Liu, X., Panagia, V., and Takeda, N. (1998) Subcellular remodeling and heart dysfunction in chronic diabetes, *Cardiovasc. Res. 40*, 239−247.
49. Godin, D. V., Lopaschuk, G. D., and McNeill, J. H. (1986) Subcellular myocardial abnormalities in experimental diabetes: role of long-chain acylcarnitines, *Can. J. Cardiol. 2*, 222−229.
50. Valianpour, F., Wanders, R. J., Overmars, H., Vaz, F. M., Barth, P. G., and van Gennip, A. H. (2003) Linoleic acid supplementation of Barth syndrome fibroblasts restores cardiolipin levels: implications for treatment, *J. Lipid Res. 44*, 560−566.
51. Broekemeier, K. M., Iben, J. R., LeVan, E. G., Crouser, E. D., and Pfeiffer, D. R. (2002) Pore formation and uncoupling initiate a Ca^{2+}-independent degradation of mitochondrial phospholipids, *Biochemistry 41*, 7771−7780.
52. Han, X., and Gross, R. W. (1990) Plasmenylcholine and phosphatidylcholine membrane bilayers possess distinct conformational motifs, *Biochemistry 29*, 4992−4996.

BI051908A